

Fine Structure and Distribution of Iridophores in the Photo-Symbiotic Bivalve Subfamily Fraginae (Cardioidea)

SHINJI ISAJI

Natural History Museum and Institute, Chiba, 955-2, Aoba-cho, Chuo-ku, Chiba, 260-8682, Japan

TERUFUMI OHNO

The Kyoto University Museum, Yoshida Hon-machi, Sakyo-ku, Kyoto, 606-8317, Japan

AND

EIJIROH NISHI

Manazuru Marine Laboratory for Science Education, Yokohama National University, Iwa, Manazuru, Kanagawa, 259-0202, Japan

Abstract. Iridophores are widely distributed in the animal kingdom. In bivalves, iridophores occur in photo-symbiotic species belonging to the subfamilies Fraginae and Tridacninae. This paper describes the fine structure and distribution of iridophores in species of Fraginae by light and electron microscopy.

Each iridophore consists of alternating layers of platelets and cytoplasm, both of about 100 nm in thickness, which is the right order for multilayer interference to occur. The iridophores occur in the hypertrophied mantle margin, including tentacles of the postero-dorsal area, and the supra-branchial chamber; these areas are exposed to sunlight when animals keep their valves open and mantle margins expanded. In addition, they also occur in the mantle lining the translucent portions of the posterior valve slope. The occurrence of iridophores appears to correlate positively with the intensity of sunlight reaching the tissues.

The iridophores may function as protectors against harmful sunlight for bivalves. They also may serve to optimize the light intensity for photosynthesis by zooxanthellae.

INTRODUCTION

Many animals have highly reflecting surfaces on various parts of their bodies. In most cases, such high reflectance is the result of thin-film interference from platelets contained in specialized pigment cells called iridophores. Iridophores contain many platelets in the cytoplasm and can reflect light with a wide range of wavelengths (Denton & Land, 1971; Land, 1972).

Among bivalves, brilliant blue or glittering white colors of the hypertrophied mantle margin of giant clams (subfamily Tridacninae; Cardioidea) are interference (structural) colors reflected by dermal iridophores (Kawaguti, 1966). The species of the Tridacninae live in shallow and warm coral reef environments, where short wavelength sunlight is predominant, and have a symbiotic relationship with photosynthetic zooxanthellae (Yonge, 1936). Their mantle margins are widely expanded and contain a great accumulation of zooxanthellae. Based on their ecology, Kawaguti (1966) proposed that the iridophores of Tridacninae might protect against harmful sunlight or supply reflected light for photoreceptive organs located on the wavy mantle margin facing the shell.

Such dermal iridophores also occur in species of Fra-

ginae (Cardioidea). These bivalves are also photo-symbiotic, live in coral reef environments, and contain numerous zooxanthellae (Kawaguti, 1968, 1983; Ohno et al., 1995). The shells of species of Fraginae are usually compressed antero-posteriorly, and are smaller and thinner than those of the Tridacninae. Their mantle margins are not widely expanded beyond the shell margins except for the tentacles (Ohno et al., 1995). Light transmission to the zooxanthellae is facilitated by translucent portions of the posterior slope of the shell. Thus, different areas of the animal receive sunlight in Fraginae than in Tridacninae. The iridophores of the Fraginae may be related to their photo-symbiotic mode of life. However, little is known about the fine structure and distribution or function of iridophores.

This paper describes the fine structure and distribution of iridophores for three species of Fraginae: *Fragum fragum* (Linnaeus, 1758), *Fragum mundum* (Reeve, 1865), and *Corculum cardissa* (Linnaeus, 1758), and provides a sound basis for understanding the function of iridophores for photo-symbiotic bivalves. The evolutionary significance of iridophores among photo-symbiotic species of Fraginae is also discussed.

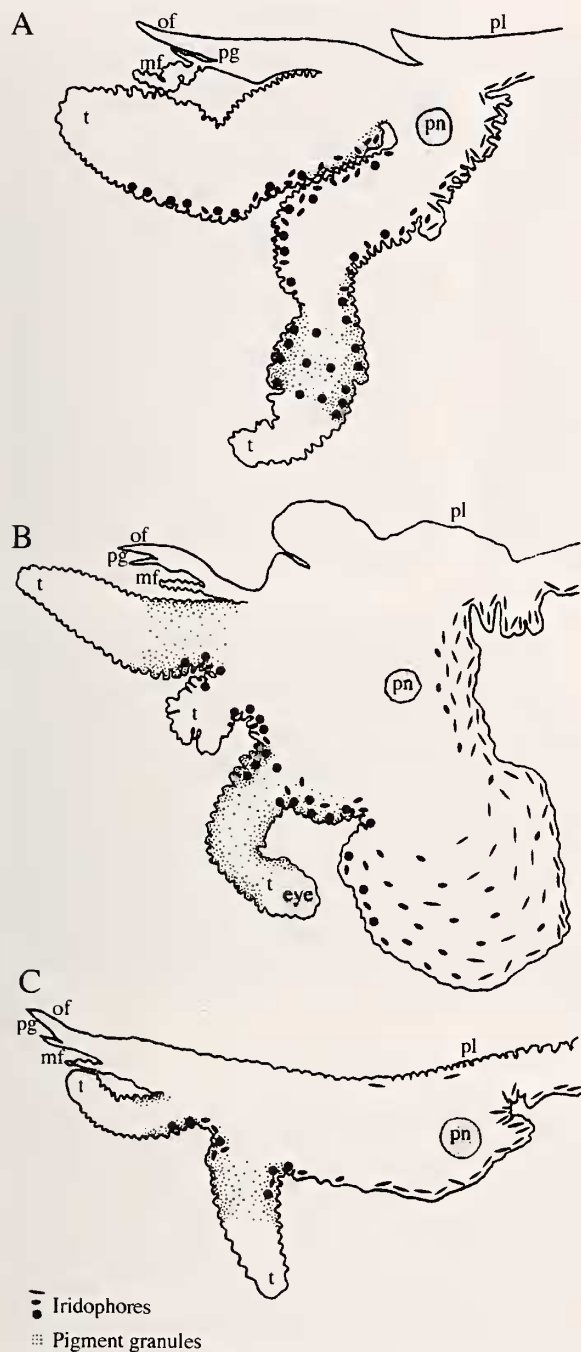


Figure 1. Semi-schematic cross sections of the mantle margin of three species of Fraginae. Three morphological types (disc-shaped, elliptical, spherical) of iridophores and pigment granules are figured. A. *Fragum mundum*. B. *Fragum fragum*. C. *Corculum cardissa*. Key: mf, middle fold; of, outer fold; pg, perios-tral groove; pl, pallial line; pn, pallial nerve; t, tentacle. Not to scale.

MATERIALS AND METHODS

Animals were collected on the shallow sand and rocky flats of Bise and Zampa, Okinawa Island, Japan, in September and December 1995.

To study the distribution of iridophores in the mantle margins, specimens of three species (six individuals of *F. fragum*, seven individuals of *F. mundum*, and five individuals of *C. cardissa*) were kept alive in the aquarium at the Natural History Museum and Institute, Chiba. Individuals were observed with a binocular microscope when they expanded their mantle margins and tentacles fully.

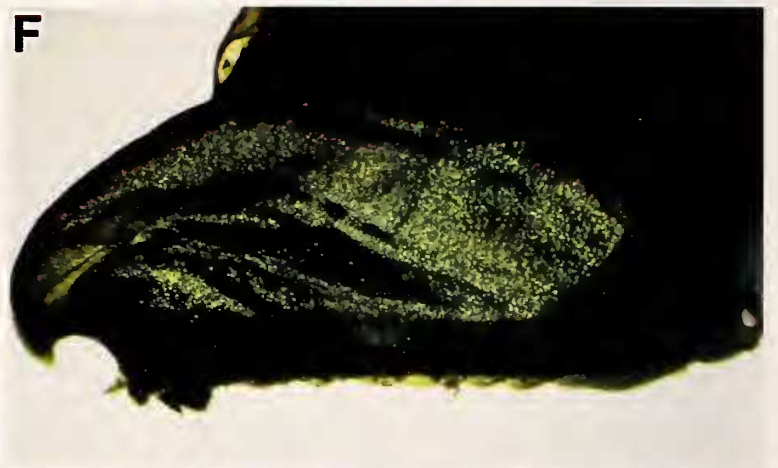
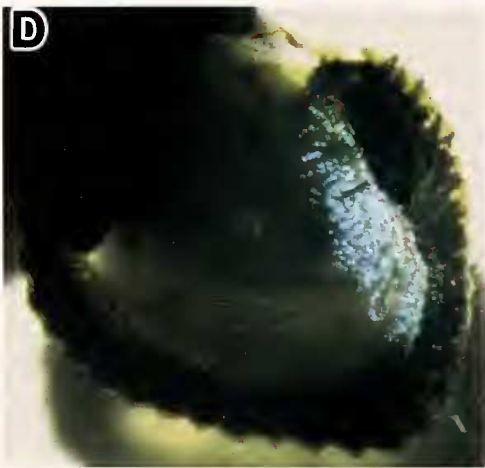
To further study the distribution of iridophores in the mantle lining the shell interior and other soft parts, specimens were fixed without sectioning into small pieces in 2% glutaraldehyde in 0.1 M cacodylate buffer (pH 7.5), and post-fixed in 0.5% osmium tetroxide for 1.5 hours in order to emphasize the contrast between iridophores and other cells. Shells were then slightly decalcified with 4.13% EDTA (pH 7.5) and removed from the soft parts for observation with the binocular microscope.

For transmission electron microscopy (TEM), small pieces (1–2 mm in thickness) were cut from two individuals of *F. fragum*, two individuals of *F. mundum*, and three individuals of *C. cardissa*, and fixed overnight in 2% glutaraldehyde in 0.1 M cacodylate buffer (pH 7.5) with 6% sucrose added for osmolarity. The tissue was then washed in cacodylate buffer for 4 hours and post-fixed in 2% osmium tetroxide for 1.5 hours. After dehydration in an ethanol series, materials were embedded in Epon 812 resin. One- μ m-thick sections were cut with a glass knife and stained with toluidine blue for light microscopy. Ultra-thin sections were cut with a diamond knife using an LKB-Ultratome and stained with uranyl acetate and lead citrate. The sections were examined and photographed with a Jeol JEM-1200EX II TEM.

All the examined specimens are stored in the Natural History Museum and Institute, Chiba (catalog numbers CBM-ZM 114503, 114504, 114505). The taxonomic assignments made in this paper are based on Schneider (1992, 1998).

SHELL FORMS AND LIFE HABITS

The shell forms and life habits of the three species examined differ from each other. *Fragum fragum* attains about 35 mm in PSL (= posterior slope length: umbo to postero-ventral corner). It lives in calcareous, bioclastic sand flats and immerses the valves completely in the sediment. The tentacles secrete mucus, and sand grains adhere to them. In the natural life position of *F. fragum*, only the exhalant and inhalant siphons and a part of the posterior mantle margins covering the shell gape are exposed above the sediment surface (Ohno et al., 1995). This infaunal mode of life results in a clean posterior shell surface with no epibionts.



Fragum mundum is a small (maximum PSL < 10 mm) epifaunal species. It lives in intertidal rocky flats, attaching to algae with mucus, and immerses only the anterior part of the shell in algal mats or shallow sediments. The posterior shell surface is usually covered by epibionts. The shell form of *F. mundum* is similar to that of *F. fragum*, but the former has a more acute angle between the posterior and ventral valve margins.

Corculum cardissa attains about 50 mm in PSL. It is also epifaunal on sand flats. The shell is greatly expanded in width but extremely compressed antero-posteriorly. The posterior shell surface of the specimens living on intertidal sand flats is usually covered by abundant epibionts, whereas those living in subtidal zone have few epibionts.

The shells of the three species are composed of a mosaic of translucent and non-translucent domains. The most translucent domains (windows) are located on the posterior valve slope of each species. In *C. cardissa*, there are various interpretations of the microstructure of the translucent windows proposed by Vogel (1975), Watson & Signor (1986), and Seilacher (1990). Carter & Schneider (1997) reconciled the various interpretations. According to them, the non-translucent domains of the posterior valve slope of *C. cardissa* consist of a fibrous prismatic (FP) outer, branching crossed lamellar (BCL) middle, and irregular complex crossed lamellar (ICCL) inner layers. At the translucent window, the FP outer layer penetrates deeply into the more opaque BCL middle shell layer. Deeper in the windows, such FP structure passes into a dissected crossed prismatic (DCP) structure which forms a planoconvex lens. This modification of the BCL middle shell layer into a more translucent DCP structure is effective to enhance light transmission toward the shell interior (Carter & Schneider, 1997).

In *F. mundum*, the posterior shell windows are as clear as those of *C. cardissa*. The non-translucent domains are milky white in color. Therefore there is high contrast between these two domains. The translucent windows are composed of the needlelike outer crystallites in contrast to the crossed lamellar outer shell layer of the non-translucent domains.

In contrast, the posterior shell windows of *F. fragum* are less translucent than those of the other two species.

The windows are composed of needle-shaped outer crystallites and a complex crossed lamellar inner layer. The needle-shaped outer crystallites radiate, and those of the complex crossed lamellae in the inner shell layer are differently oriented from one lamella subunit to another (Ohno et al., 1995). Thus, light penetrating into the shell of *F. fragum* is scattered by these two layers.

RESULTS

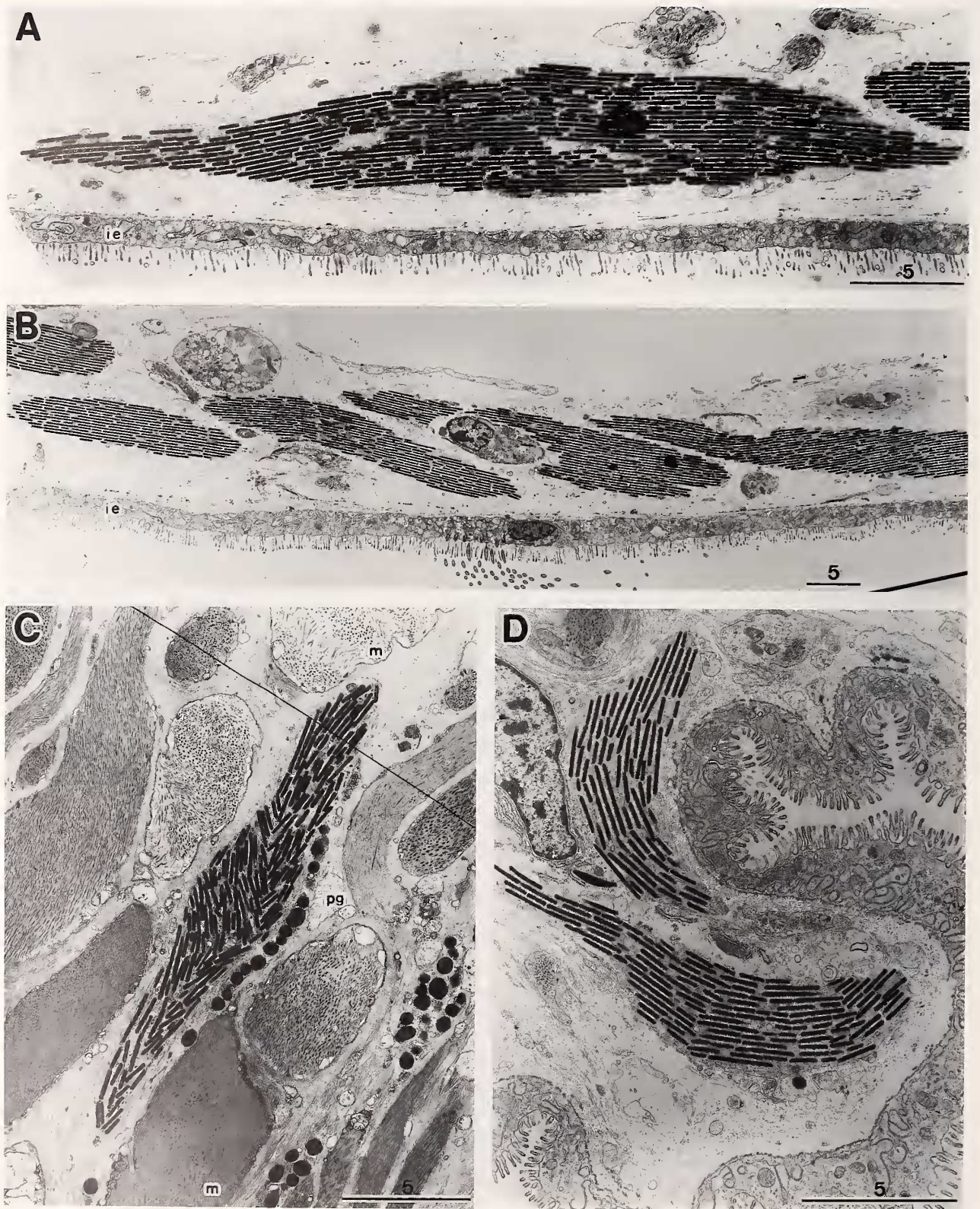
Gross Morphology of the Mantle Margin

The morphology of the mantle margin was similar in all three examined species. There were three folds at the mantle margins. The outer and middle folds were relatively small; the inner fold, which bore the tentacles, was hypertrophied (Figure 1).

In *F. fragum* and *F. mundum*, the inner fold was furnished with numerous tentacles and was moderately hypertrophied, especially ventral to the inhalant siphon. In *F. fragum*, the tentacles lay somewhat parallel to the surface of the posterior valve slope when they extended fully (Figure 2A), whereas those of *F. mundum* were often expanded at a more or less perpendicular angle to the surface of the posterior valve slope (Figure 2B). In these species, the fully expanded tentacles around the two siphons were as long as the shell width. In addition, these two species widely exposed their hypertrophied mantle margins around the postero-ventral corner of the shell (Figure 2A,B). In contrast, the inner mantle fold of *C. cardissa* was less hypertrophied, and the tentacles were slender and considerably shorter in comparison with their body size. These inconspicuous tentacles extended from the very narrow posterior shell gapes (Figure 2C,G).

Some tentacles around the two siphons of *F. fragum* bore what appeared to be photoreceptive structures; similar structures were not observed in *F. mundum* and *C. cardissa*. The eye-bearing tentacles were more or less shorter than plain tentacles. Mucus cells took the place of the photoreceptive organs in the latter. The photoreceptive structures were composed of lens cells, retinal cells, and ciliated cells. Detailed information on the fine structure of these will be presented in a separate paper.

Figure 2. Light micrographs showing the iridescent colors reflected by iridophores in living (A, B, C, G) and fixed (D, E, F) specimens. A. *Fragum fragum* (11 mm in PSL), showing red iridescent color in the tentacles. B. *Fragum mundum* (4 mm in PSL), showing red iridescent color penetrating through the translucent window (arrow head). C. *Corculum cardissa* (30 mm in PSL), showing few epibionts on the shell surface. D. *F. fragum* (8 mm in PSL, CBM-ZM 114503), showing the accumulation of iridophores in the postero-ventral area of the mantle. E. *F. mundum* (same specimen as in B, CBM-ZM 114504), showing the iridophores located exactly beneath the translucent windows (arrow heads). F. *C. cardissa* (same specimen as in C, CBM-ZM 114505), showing the banded arrangement of the iridophores. G. Enlarged view of posterior edge of *C. cardissa* in C, showing red iridescent color penetrating through the translucent windows. Arrow heads indicate the pigment granules in a tentacle.



Fine Structure of Iridophores

The fine structure of the iridophores was almost identical in the three species. The shape of iridophores showed some variation in relation to their location. Iridophores located in the mantle near the pallial nerve and inside of the pallial line were always disc-shaped, and attained about 50 μm in maximum diameter (Figures 1, 3A, B). Sometimes the shape of these iridophores were slightly modified near the epithelium (Figure 3D). In contrast, iridophores located in the mantle folds, especially in the basal part of the tentacles, were often elliptical to spherical in shape and about 10–15 μm in maximum diameter (Figures 1, 4A, B).

Disc-shaped iridophores contained a stack of 20–30 platelets. Platelets of neighboring stacks were arranged parallel to each other (Figure 3A, B). Each platelet was bound by a double membrane and separated from the next platelets by an approx. 100 nm-thick layer of cytoplasm (Figure 5C). Each platelet was rectangular in shape with truncated or rounded corners (Figure 5B), and measured about 2–3 $\mu\text{m} \times 1$ –2 μm ; and was about 100 nm thick. The platelets had an almost uniform electron density, except for occasional platelets in the intermediate stage of organellogenesis that occurred near the nucleus of disc-shaped iridophores (Figure 5A). The nucleus was usually located peripherally; and rough endoplasmic reticula, microtubules, mitochondria, and Golgi bodies were occasionally observed in the disc-shaped iridophores (Figure 5A).

In contrast, in the iridophores located in the tentacles, the platelets were arranged in a somewhat irregular manner (Figure 4A,B). Such an irregular arrangement of platelets sometimes also occurred in disc-shaped iridophores (Figure 3C). No apparent organelles such as nucleus, rough endoplasmic reticulum, or Golgi bodies were observed, nor were intermediate stages of organellogenesis of platelets seen. Isolated platelets were also found extracellularly around the elliptical to spherical iridophores, especially in the tentacles (Figure 4C,D).

Distribution of Iridophores

Iridophores were mainly distributed in the connective tissues beneath the epithelium of the inner mantle fold of the postero-dorsal area. They also occurred in the postero-dorsal area of the supra-branchial chamber. Both the mantle margin and the supra-branchial chamber were observed in living specimens when animals kept their valves open and mantle expanded (Figure 6: dotted area).

In these areas, the iridophores were usually tinged with yellowish brown to red iridescent colors in seawater under fluorescent lighting (Figure 2A). The same distributional pattern of iridophores was found in the three examined species regardless of shell size.

In the mantle margin, the disc-shaped iridophores were most abundantly located at the proximal portion of the inner fold, just beneath the epithelium around the pallial nerve (Figure 1). They were usually arranged parallel to the basal surface of the mantle epithelium (Figures 1, 3D). Large numbers of disc-shaped iridophores were found in the hypertrophied inner fold. These disc-shaped iridophores gradually decreased in abundance toward the tentacles, while spherical iridophores and isolated platelets gradually became more abundant distally in the inner mantle fold (Figure 1). The spherical iridophores appeared to be arranged more or less at random with respect to the basal surface of the mantle epithelium. In the tentacles, they were concentrated basally, but almost absent distally, especially at the tentacle tip (Figure 2A). Only occasional isolated platelets occurred in the distal part of tentacles (Figure 4C,D). These appeared to be a gradual transition from disc-shaped to elliptical and then into spherical iridophores, with an apparent breakdown of cell bodies and release of free platelets at the culmination of this trend.

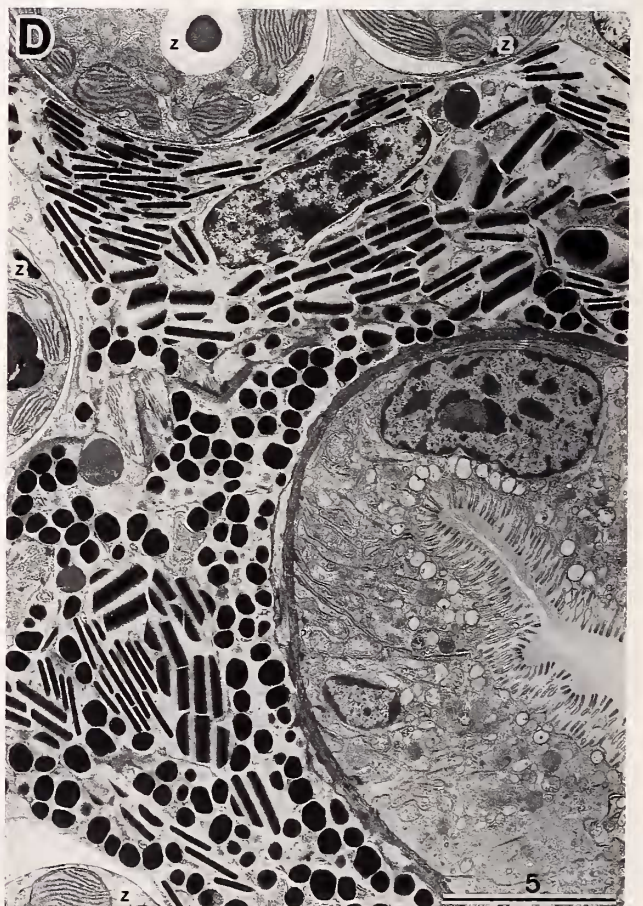
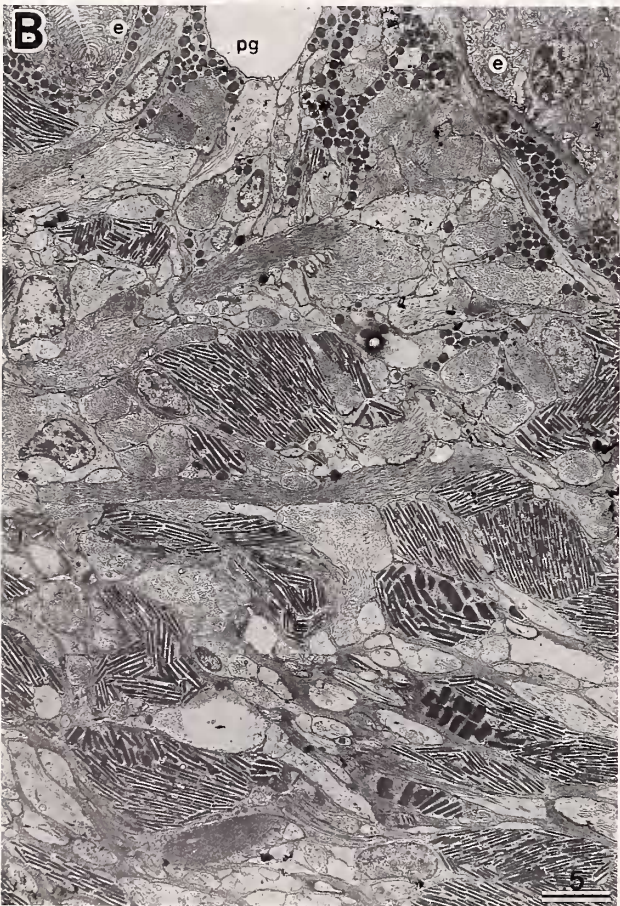
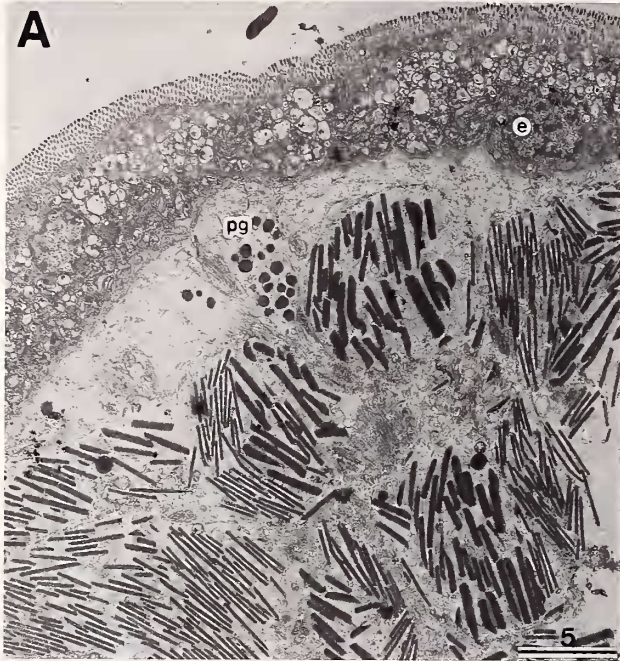
Iridophores in the tentacles were usually accompanied by numerous pigment granules (= "melanophores" in Kawaguti, 1966). These pigment granules were tinged with whitish silver colors and occurred in distinct bands along the tentacle (Figures 2G: arrow heads). They lay in the connective tissues just beneath the epithelium (Figures 4B, D, 5E). Granules were polygonal and about 0.8 μm in diameter (Figure 5D), and showed almost uniform electron density. Although disc-shaped iridophores were abundant, pigment granules were not observed in the proximal portion of the inner mantle fold (Figure 1).

There were also abundant disc-shaped iridophores in the mantle inside the pallial line of the postero-dorsal area, just beneath the translucent shell windows in some specimens. They were always arranged parallel to the basal surface of the mantle epithelium (Figures 1, 3A, B). The occurrence of iridophores in this area showed variation with shell size and transparency.

Four small specimens of *F. fragum* (5.0, 8.0, 11.0, 11.5 mm in PSL, respectively) examined had iridophores in the mantle inside the pallial line, especially beneath the exhalant siphons. Figure 2D showed numerous irido-

←

Figure 3. TEM of iridophores in the mantle of *Corculum cardissa* (A, B, C) and *Fragum mundum* (D). A. Disc-shaped iridophore located in the inside of the pallial line. B. Imbricated iridophores located near the pallial line. C. Iridophore surrounded by pallial muscles. D. Iridophores located beneath the inner epithelium near the pallial nerve. Key: ie, inner epithelium; m, muscle; pg, pigment granules. Scales in micron.



phores occurring in the mantle inside the pallial line lining the posterior valve slope of a small specimen (8.0 mm in PSL). This specimen showed the most dense iridophores in the area among four small specimens, whereas the smallest one (5.0 mm in PSL) had less dense iridophores in the corresponding area than this specimen. In contrast, no iridophores were observed in the mantle inside the pallial line in two larger specimens (14.0, 29.0 mm in PSL). The shells of these larger specimens were much thicker, and their posterior valve slopes were milky white in color and less translucent than those of the smaller ones.

Among *F. mundum* examined (about 4.0 to 6.0 mm in PSL), red iridescent color was observed through a translucent window of the posterior valve slope (Figure 2B). Iridophores were locally restricted to the mantle lining the translucent windows (Figure 2E).

In all specimens of *C. cardissa* examined, iridophores were observed in the mantle lining the posterior valve slope inside the pallial line. Yellowish brown to red iridescent colors were observed through the translucent windows in a small (30 mm in PSL) specimen collected from the subtidal zone (Figure 2C, G). This specimen had abundant iridophores on the posterior slope of the mantle, concentrated in bands that appeared to correspond to the radial ribs on the shell surface (Figure 2F). In contrast, specimens heavily fouled with epibionts had relatively few iridophores, usually restricted to a narrow band along the newly formed shell margin, where epibionts were less abundant than in the older part of the shell. Numerous iridophores also occurred in the mantle lining the anterior side of the shells carina, where the shell was most compressed antero-posteriorly.

Distribution of Zooxanthellae

In all three species examined, zooxanthellae occurred intercellularly in almost all parts of the anatomy. Zooxanthellae were most common inside the shell, especially in the ctenidia, and less common in the exposed parts of the mantle, including the tentacles.

In *F. fragum* and *F. mundum*, zooxanthellae were found in the ventral mantle margins just near the postero-ventral corner. Abundant zooxanthellae also existed within the mantle inside the pallial line along the posterior valve margins and posterior part of the ventral margin. Abundance of zooxanthellae gradually decreased toward the anterior in the mantle. Details of distribution of zoo-

xanthellae in *F. fragum* were described by Ohno et al. (1995).

In contrast to *Fragum* species, *C. cardissa* contained only a few zooxanthellae within the mantle lining the posterior valve slope both outside and inside the pallial line. The mantle lining the anterior valve slope, on the contrary, contained abundant zooxanthellae.

DISCUSSION

Reflecting System of Iridophores

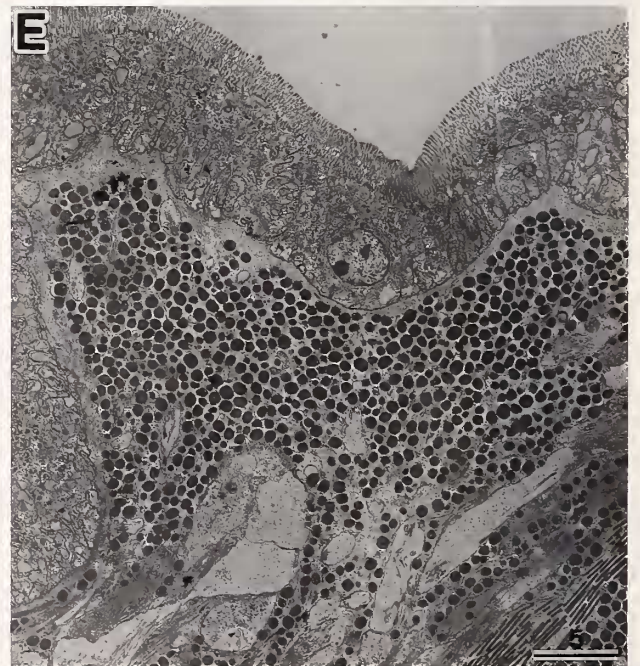
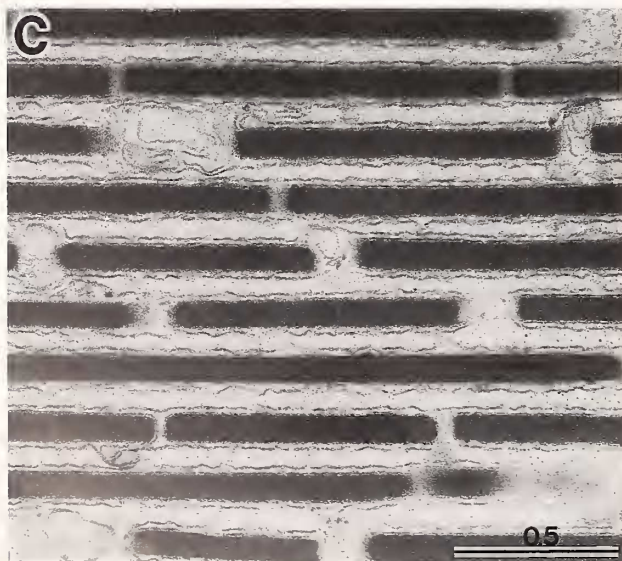
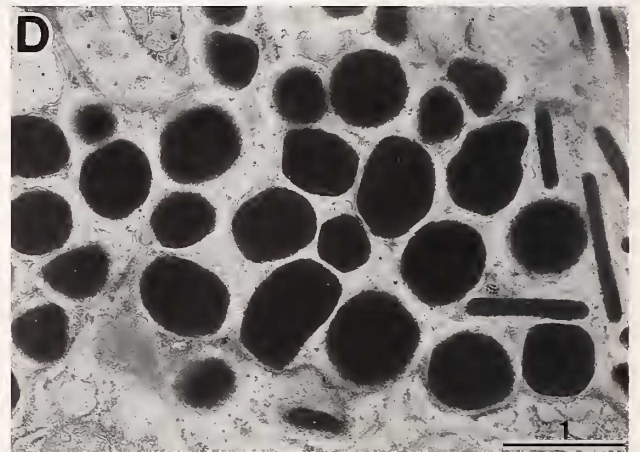
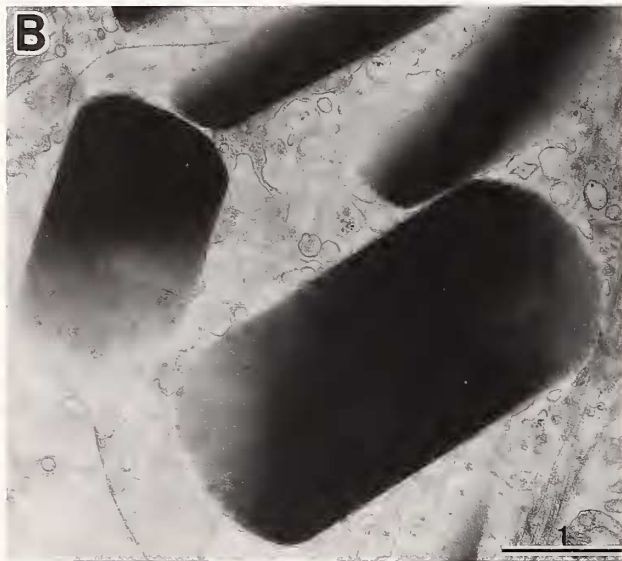
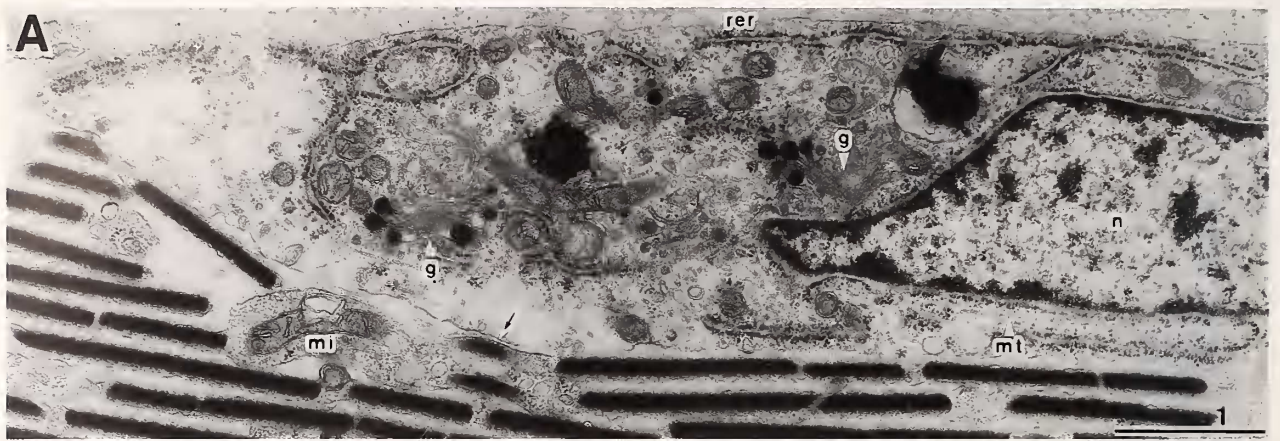
The fine structure of disc-shaped iridophores, such as apparent organella, regular arrangement of platelets, and intermediate stages of organellogenesis of platelets indicates that they represent the initial stage in the differentiation of iridophores. In contrast, an irregular arrangement of platelets in the spherical iridophores and isolated platelets occurring in the distal part of the mantle margin indicates that the spherical iridophores represent the late stages in the development of iridophores, which culminates in cellular degeneration and consequent liberation of platelets. This irregular arrangement of platelets may be a result of their translocation by blood current, i.e., by expansion and contraction of tentacles. Thus, the following discussion focuses on the reflecting system of the disc-shaped iridophores.

The iridophores consist of alternating layers of platelets and cytoplasm, both about 100 nm in thickness, whose refractive indices are high and low, respectively. This thickness is appropriate for multilayer interference to occur. Huxley (1968) showed that the highest reflectivity of a multilayer system at a given wavelength λ_0 would be given if these alternate layers all had an optical thickness of $\frac{1}{4} \lambda_0$. Many biological reflectors, e.g., those found in the integuments and eyes of fish and cephalopods, closely approach such an "ideal" quarter wavelength arrangement (Denton & Land, 1971; Land, 1972).

Assuming that the iridophores examined here are "ideal" quarter wavelength reflectors, the highest reflectivity is calculated from the formula $\lambda_{\max} = 4 n_a d_a$ where n_a is refractive index of platelet and d_a is actual thickness of platelet, which is nearly equal to the thickness of the inter-platelet cytoplasmic layer. Although chemical composition of the platelets of *Fraginæ* is not examined in the present study, they seem to be composed of chitin or some solid insoluble protein, since they do not shatter or disappear in preparation for electron microscopy as they

←

Figure 4. TEM of iridophores located in the tentacles of *Fragum fragum* (A, B) and *Fragum mundum* (C, D). A. Spherical iridophores in the basal part of the tentacle. B. Spherical and irregularly shaped iridophores surrounded by muscles in the basal part of the tentacle. C. Isolated platelets in the distal part of the tentacle. D. Isolated platelets beneath the epithelium of the tentacle. Note the pigment granules in all pictures. Key: e, epithelium; pg, pigment granules; z, zooxanthellae. Scales in micron.



do in both *Pecten* and fish materials, which are composed of guanine (Barber et al., 1967; Denton & Land, 1971; Land, 1972). Taking the refractive index of platelets as those of chitin or dry protein (e.g., keratin): $n_a = 1.56$ (Land, 1972), a peak reflectance is estimated at $4 n_a d_a = 624$ nm. In fact, yellowish brown to red iridescent colors were reflected by iridophores in living specimens (Figure 2A,B,G). This indicates that the multilayer system of iridophores is close to being an "ideal" quarter wavelength reflector.

In all iridophores examined, the platelets were uniform in thickness. Thus, variation in the observed colors must be attributed largely to differences in inter-platelet spacing. Changes in iridescent color from yellowish brown or red in living animals (Figure 2B, G) into greenish yellow following fixation (Figure 2E, F) must be due to shrinkage of inter-platelet space. It can not be attributed to the refractive index of ethanol (1.36), which is close to that of seawater (approx. 1.34). In addition, irregular arrangement of platelets in the spherical iridophores and isolated platelets in the connective tissues results in different reflective colors from those of the disc-shaped ones.

Distribution of Iridophores

Light appears to be the main factor determining the distribution of iridophores in the mantle inside the pallial line.

In *F. fragum*, iridophores were common in the postero-dorsal part of the mantle in small specimens, but absent in the largest specimen examined. In *F. mundum*, iridophores were concentrated in the mantle exactly beneath the translucent windows. In *C. cardissa*, the banded arrangement of iridophores in the posterior half of the mantle was observed in the specimen with few epibionts on the shell surface. Thus, the distribution of iridophores shows good correlation with shell transparency. This suggests that light is an important control in the development of iridophores. It also implies that iridophores may disappear with growth unless they receive the sufficient amount of sunlight.

Functional Significance of Iridophores

Iridophores are distributed in the eyes and the integuments of numerous animals (Denton & Land, 1971; Land, 1972; Bubel, 1984). They invariably have a multilayer structure consisting of alternating layers with high and

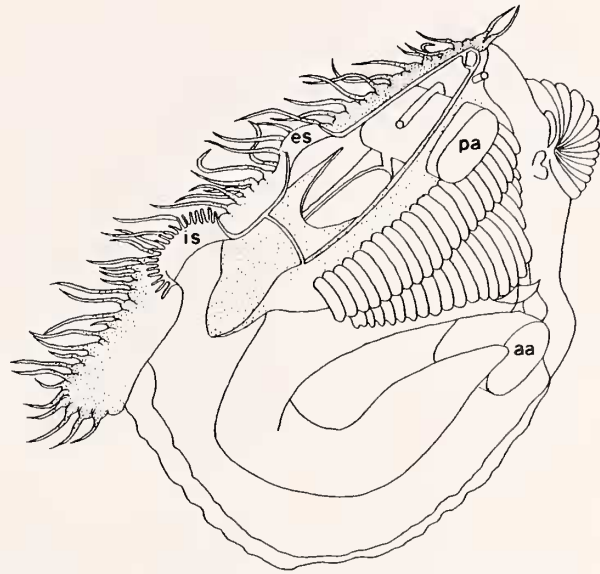


Figure 6. Schematic figure of *Fragum fragum* showing the anatomy and occurrence sites of iridophores (dotted area). Key: aa, anterior adductor muscle; es, exhalant siphon; is, inhalant siphon; pa, posterior adductor muscle. Modified from the text-fig. 2 in Ohno et al. (1995).

low refractive indices. They can serve many functions. Multilayer reflectors, for example, are found in many vertebrate and molluscan eyes as tapetal reflectors (Denton, 1971; Barber et al., 1967). Fish and cephalopods use them as mirrorlike reflectors that serve to camouflage them and provide a display of surface color (Mirow, 1972a, b; Brocco & Cloney, 1980), or serve as reflectors in photophores (e.g., Young & Bennett, 1988).

It is obvious that the iridophores are not involved in changes of body color in species of *Fraginae* since changes of reflective color in the living animal and physiologically alterable chromatophores are not found.

In the examined species of *Fraginae*, neither photoreceptive organs nor photophores were observed in *F. mundum* and *C. cardissa*. Although *F. fragum* had eyes in the tip of the tentacles, no iridophores were present within or around them. Therefore it is also clear that the iridophores are not involved in photoreception and luminescence.

Kawaguti (1966) proposed the idea that the iridophores located in the expanded mantle of the giant clam *Tridacna gigas* (Linnaeus, 1758) reflect the sunlight to eyes on

Figure 5. TEM of iridophores and pigment granules of *Corculum cardissa* (A, C), *Fragum fragum* (B, E), and *Fragum mundum* (D). A. Intermediate stage of organellogenesis of iridosomal platelets (arrow) near the nucleus. B. Horizontal section through platelets. C. Vertical section through a stack of platelets of the disc-shaped iridophore. D. Pigment granules in the tentacle. E. Accumulation of pigment granules beneath the epithelium of the basal part of tentacle. Key: g, Golgi body; mi, mitochondria; mt, microtubule; n, nucleus; rer, rough endoplasmic reticulum. Scales in micron.

the mantle margin and this may facilitate the animals response to changes of brightness in the environment. This possible role does not apply here because the iridophores located in the tentacles are fewer than those of the giant clam and are usually covered by sand grains in *F. fragum*.

Although the species examined lack an association between iridophores and photoreceptive organs, *Cerastoderma edule* (Linnaeus, 1758) of the closely related subfamily Lymnocardinae has iridophores in the tentacle eyes. Barber & Wright (1969) revealed that the iridophores of *C. edule* function as photoreceptive reflectors. The shape of platelets in the iridophores of *C. edule* is similar to those of *Fraginae*. This resemblance may be due to a similar chemical composition of the platelets in the two groups. It is noteworthy that these closely related groups evolved the same type of iridophore for different functions.

There is a general agreement that the postero-dorsal shell of the *Fraginae* became translucent to supply light for zooxanthellae (Watson & Signor, 1986; Ohno et al., 1995; Carter & Schneider, 1997). However, such shell transparency may result in an oversupply of harmful light to bivalves. Judging from the distribution of iridophores within the mantle inside the pallial line, it seems that the penetration of light in translucent portions of the shell is effectively reduced by reflection of iridophores. Thus, the prime function of iridophores may be to reflect excessive and harmful light in the tropical coral reef environments, where short wavelengths predominate. This reflection may allow the optimal amount of light to reach the bivalves.

However, such a screening effect by the iridophores may be disadvantageous for the photosynthesis of zooxanthellae. Zooxanthellae need sufficient light for photosynthesis. However, zooxanthellae were not concentrated in the mantle just beneath the translucent shell windows but occurred in the gill leaflets where iridophores were not observed. Moreover, in *C. cardissa*, which had the most translucent shell, zooxanthellae were most common in the anterior mantle, i.e., farthest from the impinging light; the accumulation of zooxanthellae is not common in the brightest area within the mantle. This phenomenon might be explained by "shade adaptation" of zooxanthellae, meaning molecular level adaptation to enable photosynthesis in low light intensity (Falkowski & Owens, 1980). Ohno et al. (1995) reported that the compensation point of photosynthesis of the zooxanthellae of *F. fragum* is one-quarter that of the zooxanthellae of the epifaunal *Tridacna maxima* (Röding, 1798) (Scott & Jitts, 1977), and indicated shade adaptation for the zooxanthellae of *F. fragum*. It seems reasonable therefore to suppose that this shade adaptation of zooxanthellae influenced the distribution of zooxanthellae within the soft parts of *Fraginae*.

Another explanation for zooxanthellae to avoid living in a brightly lit area is to reduce the impact of harmful

ultraviolet radiation. Gleason & Wellington (1993) reported that increased ultraviolet radiation in clear water induced coral bleaching (the loss of zooxanthellae) at depths greater than 20 m in the absence of abnormally high seawater temperatures. At such depths, zooxanthellae living within the coral reported by them may be shade-adapted species. Thus, it is likely that shade-adapted zooxanthellae avoid not only high light intensity but also ultraviolet light. It is also likely that iridophores may provide possible screening against ultraviolet light as well as optimize light intensity, and thus provide shade-adapted zooxanthellae of *Fraginae* with a more light-protected environment.

This screening effect has been demonstrated by Kawaguti (1966) for the iridophores of the giant clams (*Tridacna*). In the case of giant clams, the iridophores are associated with a great accumulation of zooxanthellae in the hypertrophied mantle. Such differences in the mode of association between iridophores and zooxanthellae in the *Fraginae* and *Tridacninae* might be due to the different ability of photosynthesis of the symbiotic zooxanthellae.

Additionally, the distal part of the tentacles had almost no iridophores in spite of their exposure to high irradiance. In this area, numerous polygonal pigment granules were located beneath the outer epithelium, which may play the role of protection against harmful sunlight instead of iridophores. In fact, the tentacles of living specimens were whitish silver in color because of the light scattered by the pigment granules.

Concluding Remarks

Regulation of light supply by refraction and scattering in the soft parts to protect the health of the animal is a plausible function of the iridophores in the *Fraginae*. It is also likely that regulatory effect provides optimum light supply for the photosynthesis of zooxanthellae.

Ohno et al. (1995) proposed that the photo-symbiosis in the *Fraginae* was initiated by the association of shade-adapted zooxanthellae and an ancestral infaunal bivalve. Because of such a point of view, a comparison with an infaunal *Fraginae* *Fragum unedo* (Linnaeus, 1758) may be helpful. Interestingly, the shell of *F. unedo* is not translucent, although the species is photo-symbiotic. Such a non-translucent shell seems to retain the ancestral form of the *Fraginae*. *F. unedo* has hypertrophied mantle margins containing many iridophores, and exposes them widely on the sediment surface to collect light (Kawaguti, 1983; Ohno et al., 1995). This association of a photo-symbiotic infaunal bivalve having a non-translucent shell and iridophore indicates that an ancestral bivalve of the *Fraginae* had iridophores in the exposed soft parts. It is likely, therefore, that iridophores have developed in order to regulate the light supply to the soft parts in the early history of a photo-symbiotic relationship between the *Fraginae* and zooxanthellae.

Since photo-symbiosis was established, photosynthesis of zooxanthellae may have worked as a selective agent that would have favored an effective light supply. In order to establish the effective light supply without risking predation, transparency of the shell may have developed. Moreover, the iridophores may have increased their important role as regulators of the light both for the bivalve itself and the zooxanthellae.

Acknowledgments. We are grateful to Dr. Terufumi Yamasu for helpful comments during a visit to the University of Ryukyus. Mrs. K. Hasegawa, Y. Nakata, D. Ohsumi, and S. Saito kindly helped us during field studies at Ryukyu Island. We wish to thank Drs. Barry Roth, Jay Schneider, and Gustav Paulay for critical review of the manuscript and for valuable comments. Thanks are also due to the Tropical Biosphere Research Center, University of the Ryukyus Sesoko Station. This study was partly financed by grant aid from the Ministry of Education, Science and Culture awarded to T. Ohno (B05454003).

LITERATURE CITED

- BARBER, V. C., E. M. EVANS & M. F. LAND. 1967. The fine structure of the eye of the mollusc *Pecten maximus*. *Zeitschrift für Zellforschung* 76:295–312.
- BARBER, V. C. & D. E. WRIGHT. 1969. The fine structure of the eye and optic tentacle of the mollusc *Cardium edule*. *Journal of Ultrastructure Research* 26:515–528.
- BROCCO, S. L. & R. A. CLONEY. 1980. Reflector cells in the skin of *Octopus dofleini*. *Cell Tissue Research* 205:167–186.
- BUBEL, A. 1984. Mollusca: Epidermal cells. Pp. 400–447 in J. Bereiter-Hahn, A. G. Matoltsy & K. Sylvia Richards (eds.), *Biology of the Integument. Volume 1: Invertebrates*. Springer Verlag: Berlin-Heidelberg-New York-Tokyo.
- CARTER, J. G. & J. A. SCHNEIDER. 1997. Condensing lenses and shell microstructure in *Corculum* (Mollusca: Bivalvia). *Journal of Paleontology* 71:56–61.
- DENTON, E. J. 1971. Reflectors in fishes. *Scientific American* 224: 64–72.
- DENTON, E. J. & M. F. LAND. 1971. Mechanism of reflection in silvery layers of fish and cephalopods. *Proceedings of the Royal Society, London A* 178:43–61.
- FALKOWSKI, P. G. & T. G. OWENS. 1980. Light-shade adaptation, two strategies in marine phytoplankton. *Plant Physiology* 66: 592–595.
- GLEASON, D. F. & G. M. WELLINGTON. 1993. Ultraviolet radiation and coral bleaching. *Nature* 365:836–838.
- HUXLEY, A. F. 1968. A theoretical treatment of the reflexion of light by multilayer structures. *Journal of Experimental Biology* 48:227–245.
- KAWAGUTI, S. 1966. Electron microscopy on the mantle of the giant clam with special references to zooxanthellae and iridophores. *Biological Journal of Okayama University* 12:81–92.
- KAWAGUTI, S. 1968. Electron microscopy on zooxanthellae in the mantle and gill of the heart shell. *Biological Journal of Okayama University* 14:1–11.
- KAWAGUTI, S. 1983. The third record of association between bivalve mollusks and zooxanthellae. *Proceedings of the Japan Academy, series B* 59:17–20.
- LAND, M. F. 1972. The physics and biology of animal reflectors. *Progress in Biophysics and Molecular Biology* 24:77–106.
- MIROW, S. 1972a. Skin color in the squids *Loligo pealii* and *Loligo opalescens*. I. Chromatophores. *Zeitschrift für Zellforschung* 125:143–175.
- MIROW, S. 1972b. Skin color in the squids *Loligo pealii* and *Loligo opalescens*. II. Iridophores. *Zeitschrift für Zellforschung* 125:176–190.
- OHNO, T., T. KATOH & T. YAMASU. 1995. The origin of algal-bivalve photo-symbiosis. *Palaeontology* 38:1–21.
- SCHNEIDER, J. A. 1992. Preliminary cladistic analysis of the bivalve family Cardiidae. *American Malacological Bulletin* 9: 145–155.
- SCHNEIDER, J. A. 1998. Phylogeny of the Cardiidae (Bivalvia): Phylogenetic relationships and morphological evolution within the subfamilies Clinocardiinae, Lymnocardiinae, Fraginae, and Tridacninae. *Malacologia* 40:321–373.
- SCOTT, B. D. & H. R. JITTS. 1977. Photosynthesis of phytoplankton and zooxanthellae on a coral reef. *Marine Biology* 41: 307–315.
- SEILACHER, A. 1990. Aberrations in bivalve evolution related to photo- and chemosymbiosis. *Historical Biology* 3:289–311.
- VOGEL, K. 1975. Endosymbiotic algae in rudists? *Palaeogeography, Palaeoclimatology and Palaeoecology* 17:327–332.
- WATSON, M. E. & P. W. SIGNOR. 1986. How a clam builds windows: shell microstructure in *Corculum* (Bivalvia: Cardiidae). *The Veliger* 28:348–355.
- YONGE, C. M. 1936. Mode of life, feeding, digestion and symbiosis with zooxanthellae in the Tridacnidae. *Scientific reports, Great Barrier Reef Expedition, British Museum* 1: 283–321.
- YOUNG, R. E. & T. M. BENNETT. 1988. Photophore structure and evolution within the Euploteuthinae (Cephalopoda). Pp. 241–251 in M. R. Clarke & E. R. Trueman (eds.), *The Mollusca. Volume 12: Paleontology and Neontology of Cephalopods*. Academic Press: London.